ELSEVIER

International Journal of Mass Spectrometry 192 (1999) 415–424

International Journal of Mass Spectrometry

Potential sputtering: desorption from insulator surfaces by impact of slow multicharged ions

F. Aumayr*, P. Varga, HP. Winter

Institut für Allgemeine Physik, TU Wien, Wiedner Hauptstrasse 8-10, A-1040 Wien, Austria

Received 27 November 1998; accepted 18 January 1999

Abstract

For certain target species, sputtering by slow multiply charged ions strongly depends on the primary ion charge state. In contrast to the usual ballistic sputtering it is not the kinetic but rather the potential energy stored in multiply charged ions that leads to this novel form of ion-induced sputtering ("potential sputtering"). A series of recent careful experiments is summarized where potential sputtering has been investigated for hyperthermal highly charged ions impact on Au, Si, GaAs, SiO_2, MgO, LiF, and NaCl. Only for alkali halides (LiF, NaCl) and to some extent for SiO_2 an enhancement of the total sputter yield, which is measured by a quartz crystal microbalance technique, with increasing charge state of the primary ion could be observed. All other targets showed only the common (collision induced) kinetic sputtering. With a defect mediated desorption model as known from electron stimulated desorption we can explain why potential sputtering is exclusively found for insulators with strong electron–phonon coupling. (Int J Mass Spectrom 192 (1999) 415–424) © 1999 Elsevier Science B.V.

Keywords: Multicharged-ion surface interaction; Hollow atoms; Potential sputtering

1. Introduction

The bombardment of solid surfaces by neutral or ionized atoms and molecules has been of continuous interest for more than a hundred years, because of many important technical applications of thereby induced processes. In most of these applications only the kinetic projectile energy is of interest as, e.g. for particle induced electron emission, ion–surface scattering and surface sputtering. However, some ion-induced phenomena can also depend on the internal (potential) energy of a projectile, and this influence will become more pronounced if this potential energy exceeds the kinetic projectile energy. In collisions of highly charged ions (HCI) with solid surfaces the large potential energy stored in these projectiles (up to several hundred kiloelectron volts) will be liberated in a small surface area of typically 100 $Å^2$ within a very short time ($\ll$100 fs). This can lead to nonlinear processes and to exotic phenomena such as, e.g. "hollow atom" formation [1–5]. The projectile potential energy may be released via electronic excitation of the target or ejection of electrons and x rays, but also by removing atoms and ions from the target surface. Although the process of kinetically induced sputtering is well established, ejection of target atoms and ions due to potential sputtering of insulators (PSI) is still almost unexplored. The use of multicharged ions for sputtering is attractive due to the possibility

* Corresponding author. E-mail: aumayr@iap.tuwien.ac.at

PII S1387-3806(99)00075-5

of achieving high sputter yields at very low kinetic impact energy. Such a "soft sputtering" would allow removing material from surfaces without producing radiation defects in deeper layers as in kinetically induced sputtering. It could thus become of considerable technological relevance: Preferential removal of insulating layers (no potential sputtering occurs for conductor surfaces, see the following) could serve for novel cleaning procedures in semiconductor industry (e.g. soft sputtering of SiO_2 from Si wafers). Other applications for nanostructuring and characteristic surface modifications of insulators are also conceivable.

In this article we will summarize a series of recent experiments where potential sputtering has been investigated for hyperthermal HCI impact on Au, Si, GaAs, SiO_2, MgO, LiF, and NaCl. For a review covering the historical development of potential sputtering see, e.g. [6]. Several reviews are available about hollow atoms and HCI–surface interaction in general [1–5]. In sec. 2, we will describe our experimental setup for measuring total sputter yields, and discuss the experimental difficulties involved. Our experimental results are summarized in sec. 3. In sec. 4, two competing models for PSI ["Coulomb explosion (CE)" versus "defect-mediated sputtering (DS")] will be presented, and in sec. 5 the available experimental evidence will be discussed with respect to these two models. This comparison does strongly favour the DS model.

2. Quartz crystal microbalance technique

To measure total sputter yields (including both neutral and ionized secondary particles) in HCI–surface collisions a sensitive quartz crystal microbalance technique has been developed at TU Wien (see, e.g. [7]). Whereas quartz crystals are widely used for determination of the area mass change and hence the thickness of deposited material, the rate for material removal has mainly been studied with other techniques such as the conventional microbalance and catcher foils analysed by Rutherford backscattering. This is not astonishing because the use of quartz

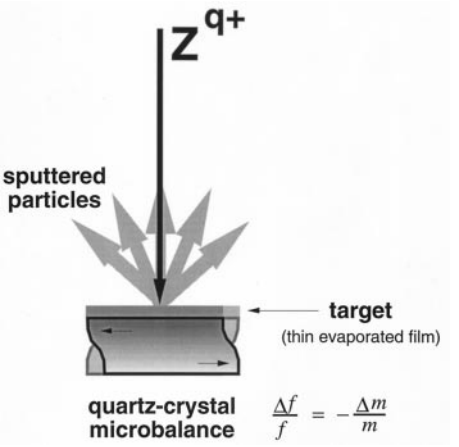

Fig. 1. Quartz crystal microbalance method (schematically; cf. text).

crystals for sputter yield measurements encounters severe problems. The rates of material removal and hence the frequency changes are rather low compared to most deposition applications, requiring high frequency stability of the crystal and of the oscillator circuit as well as high accuracy and resolution of the frequency measurement. Furthermore, a substantial amount of energy is deposited by the primary particles on the sputtered surface, causing problems due to thermal drift. In many deposition applications, the energy deposition per incident atom is only a few electron volts (sublimation energy plus heat radiation from the evaporation source). In our case the energy deposited per sputtered atom is rather in the range of up to a few hundred electron volts. Other problems arise from the sensitivity of the resonance frequency on surface stress induced by nonuniformal mass removal across the ion beam cross section. McKeown [8] was among the first to use a quartz crystal microbalance for sputtering measurements (100 eV Ar^+ on Au), and later Ellegard et al. [9] studied electron sputtering of condensed rare gases with a similar method.

We have improved this technique such that now mass changes as low as 10^{-3} monolayers for thin target films can be detected. In our setup (cf. Fig. 1) a planoconvex SC-cut quartz crystal is first coated with evaporated gold electrodes on a thin chromium adhe-

sion layer. For the measurements with LiF and NaCl a thin polycrystalline film of approximately 100 nm was evaporated from a Mo boat onto the front electrode, whereas the measurements on Au were performed by directly sputtering the quartz Au electrodes. Deposition of these electrodes and the formation with LiF and NaCl thin films on the quartz crystal faces was done in a separate high vacuum coating system (10^{-6} mbar) at approximately 150 °C substrate temperature, with deposition rates in the order of 10 nm/s. For measurements on Si and SiO_2 a pure Cr electrode was used to avoid the formation of Au silizide. Si was deposited in situ from an electron-beam heated crucible, whereas GaAs was deposited in a molecular beam epitaxy (MBE) system and transported in air to the ultrahigh vacuum (UHV) setup. SiO_2 and MgO layers have been produced in situ at an oxygen pressure of about 10^{-5} mbar by evaporation of Si and MgO, respectively.

All targets have been cleaned by sputtering and heating. To check cleanliness, quality, and stoichiometry of the thin films (especially for the alkali halides), secondary ion mass spectroscopy (SIMS), and Auger electron spectroscopy (AES) have been used in situ. Selection of the oscillator quartz crystal (cut, shape, temperature dependence of resonance frequency; see, e.g. [10,11]) is of great importance for achieving highest possible mass resolution.

Since the deposited film is very thin compared to the thickness of the quartz crystal, it is sufficient to use the simple equation

$$\frac{\Delta m}{m} = -\frac{\Delta f}{f} \tag{1}$$

that relates the relative mass loss $\Delta m/m$ to the relative change of frequency $\Delta f/f$.

To determine the total sputter yield in dependence of the HCI kinetic energy, one has to consider two important facts which can strongly influence the results. The first point concerns the measurement of the primary ion current. We used a biased Faraday cup to reduce the influence of ion induced electrons. Second, the energy dependent influence of primary ion deposition in the first monolayers at low ion dose influences directly the frequency change in the opposite sense of the sputtering effect until steady state conditions are reached.

For LiF we have assured at 100 eV Ne^+ bombardment that measurements were performed under steady-state conditions. After a Ne^+ ion dose of 1×10^{16} ions/cm^2, which corresponds to the removal of two monolayers, there was no significant change in the sputtering rate within an accuracy of 10%.

Our technique does not suffer from the problems inherent to collection of sputtered particles (e.g. incompletely defined collection geometry and/or neutral particle sticking coefficients), since the total sputter yields can be readily determined from the frequency change for a known ion current density. High stability of the resonance frequency [$\sim$1 mHz root mean square (rms) frequency noise at 6 MHz] was achieved by operating the quartz crystals within $\pm$0.1 °C of the minimum of their frequency versus temperature curve at 190 °C, which means that also the LiF target film has to be kept at this temperature. Influence of thermal stress arising from temperature gradients due energy deposition by incoming ions has been strongly reduced by using SC-cut crystals for which the resonance frequency is most insensitive to radial stress.

Finally, we would like to recall specific experimental difficulties which can be encountered when studying the interaction of charged particles with insulating targets. In general, influence of the charge state of the projectile (i.e. its potential energy represented by the total ionization energy of the respective neutral atom) becomes most effective at the lowest impact velocity where processes due to the kinetic projectile energy will be drastically reduced or absent altogether. A basic requirement for reproducible results which can be compared with available theories are clean and well characterised surfaces. In the case of polycrystalline targets also structural properties cannot be neglected. Both for semiconductor- and insulator surfaces sputtering and annealing as commonly applied to metal targets are less effective or even destructive. The extreme sensitivity of oxides to ion bombardment causes preferential sputtering of oxygen in the near surface region, which severely modi-

fies surface properties. Another difficulty in such ion beam experiments is the possible charging of the target surface. Both primary ions and ejected electrons give rise to a positively charged surface layer which not only will influence the effective ion impact energy and beam geometry, but also the energy distribution of emitted charged particles. Since secondary ions as well as ejected electrons involve kinetic energy maxima at a few electron volt only, target charging by only a fraction of a volt can strongly influence the total yields. Special precautions are needed to overcome such difficulties (e.g. electron flooding, deposition of insulator target material as ultra-thin films on metal substrates, heating of samples up to a temperature where ion conduction becomes sufficiently large, as in the case of alkali halides).

3. Experimental results

With the method described in sec. 2, sputtering measurements have been carried out for the impact of Ar^{q+} ions up to $q = 9$ from a 5 GHz electron cyclotron resonance (ECR) ion source [12] on various surfaces as Au (a metal), alkali halides (LiF and NaCl), oxides (SiO_2, MgO), and semiconductors (Si, GaAs). To investigate projectile ions in higher charge states (Ar^{q+} ions up to $q = 14$ and Xe^{q+} ions up to $q = 27$) our apparatus was moved to the 14.5 GHz ECR ion source at HMI Berlin (collaboration with N. Stolterfoht and co-workers).

Dependences of the measured total sputter yields Y on projectile kinetic energy E_k have been plotted in Figs. 2–8 for the different targets under investigation (data from [13–16]). Obviously for LiF (Fig. 2), NaCl (Fig. 3), and to a somewhat smaller extend for SiO_2 (Fig. 4) the total sputter yield increases dramatically with increasing charge state (with a record high neutral sputtering yield of approximately 300 LiF molecules per Xe^{27+} ion). In addition, for these targets a considerable sputtering yield can be observed down to very low impact energies (≥5xq eV) with no apparent impact energy threshold as in the case of kinetic sputtering. For all other targets (see

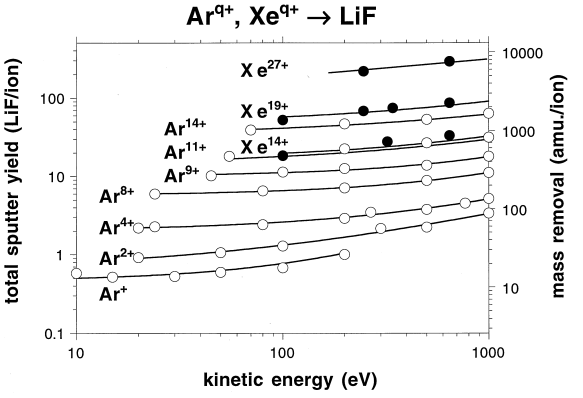

Fig. 2. Experimentally determined total sputter yield (left scale) and actually measured mass removal (right scale) per incident Ar^{q+} (open symbols) and Xe^{q+} (closed symbols) as a function of ion impact energy. Data from [16] (solid lines for guidance only).

Fig. 5 for Au, Fig. 6 for Si, Fig. 7 for GaAs, and Fig. 8 for MgO) the potential energy does not influence the sputtering yields at all, and total sputter yield dependences on impact energy are as for kinetic sputtering where momentum transfer is the dominant mechanism. Accompanying secondary ion yield measurements of F^-, F^+, and Li^+ for LiF showed that the sputter yield is dominated by neutrals (cf. Fig. 9) which are at least two orders of magnitude more abundant than secondary ions [17]. Yields of molecular ions, such as Li_2^+, LiF^+, LiF^-, Li_2F^+, LiF_2^-, are approximately 2–3 orders of magnitude smaller. This

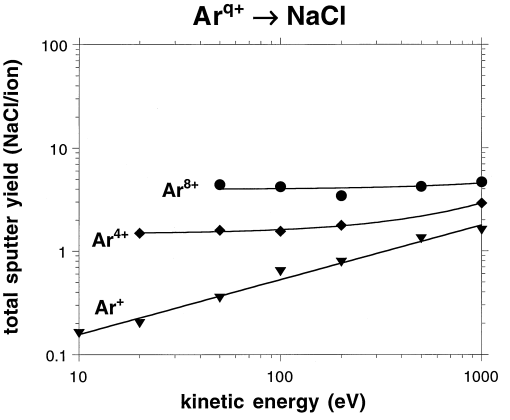

Fig. 3. Experimentally determined sputter yield for Ar^{q+} ion impact on NaCl as a function of ion impact energy. Data from [14] (solid lines for guidance only).

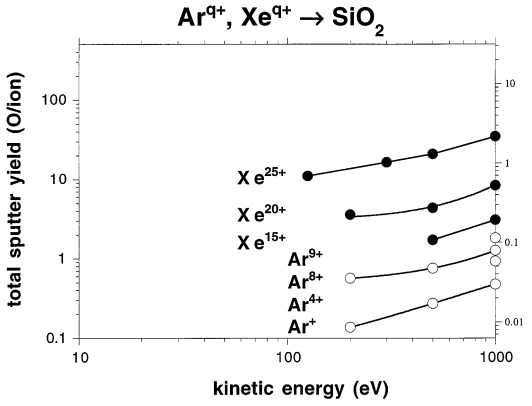

Fig. 4. Experimentally determined sputter yield for Ar^{q+} and Xe^{q+} ion impact on SiO_2 as a function of ion impact energy. Data from [16] (solid lines for guidance only).

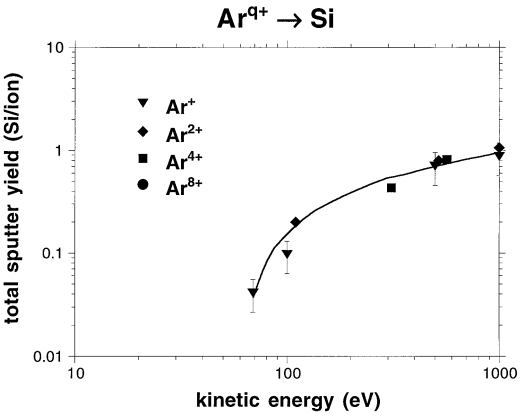

Fig. 6. Experimentally determined sputter yield for Ar^{q+} ion impact on Si as a function of ion impact energy. Data from [14] (solid line for guidance only).

behaviour is expected to be characteristic for other alkali halides as well.

For the impact of slow Ar^{q+} on SiO_2 the potential sputtering effect was found to be dose dependent, i.e. the apparent yield decreased with increasing ion dose, indicating preferential sputtering of oxygen. By contrast, for LiF and NaCl surfaces stoichiometric sputtering was found. Table 1 summarises the experimental dependences of potential sputtering yields on the target materials investigated.

4. Coulomb explosion versus defect mediated sputtering

Our current understanding of the interaction of slow HCI with metal surfaces is based on the "classical over-the-barrier" model [2,3,18], the main features include acceleration of the HCI towards the metal surface by its own image charge, and resonant transfer of conduction band electrons into highly excited electronic states of the projectile (Fig. 10). This results in the transient formation of very short lived "*hollow atoms*," where outer Rydberg orbitals

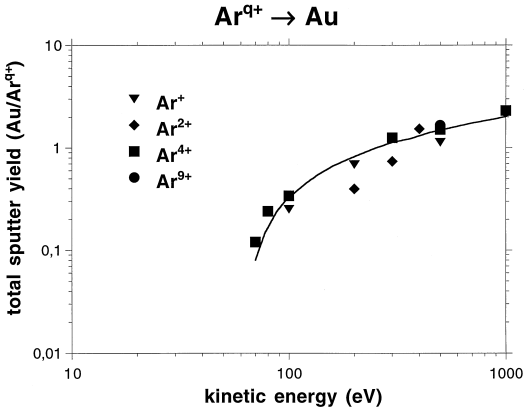

Fig. 5. Experimentally determined sputter yield for Ar^{q+} ion impact on Au as a function of ion impact energy. Data from [14] (solid line for guidance only).

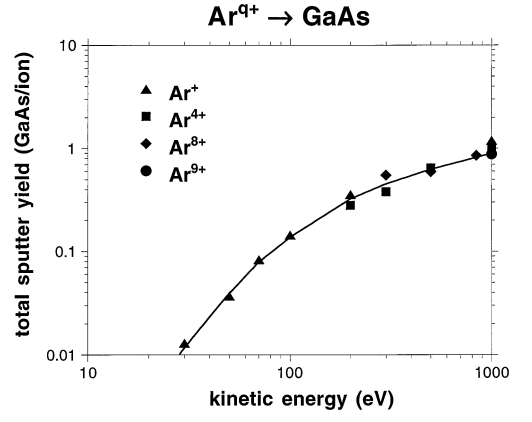

Fig. 7. Experimentally determined sputter yield for Ar^{q+} ion impact on GaAs as a function of ion impact energy. Data from [14] (solid line for guidance only).

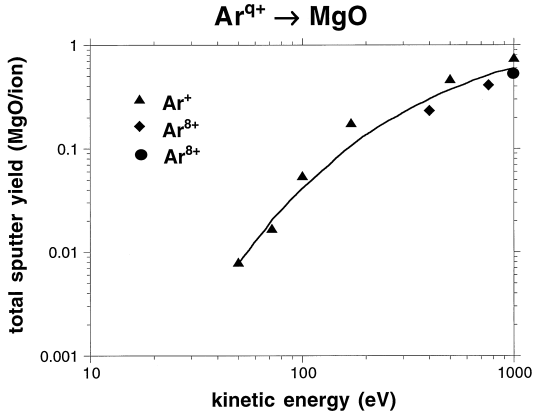

Fig. 8. Experimentally determined sputter yield for Ar^{q+} ion impact on MgO as a function of ion impact energy. Data from [14] (solid line for guidance only).

are transiently populated and inner shells can stay empty. Although the projectiles become completely neutralised in front of the surface and excited states decay rapidly by autoionisation via ample emission of low energy electrons [19], only a fraction of the potential energy originally stored in the projectile is released above the surface, because the image charge attraction limits the available interaction time. A large part of this potential energy can thus only be liberated in close vicinity of or even below the surface, when Rydberg electrons have been "peeled off" and more

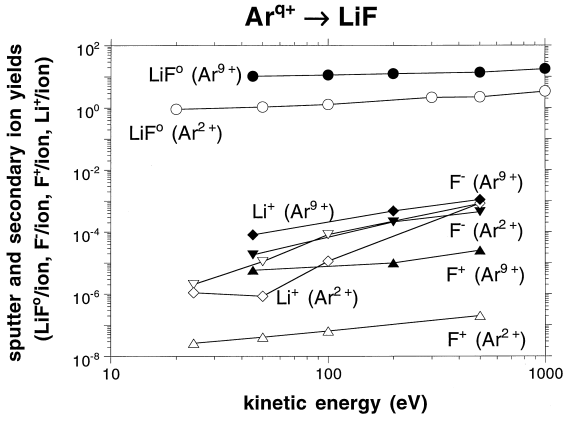

Fig. 9. Experimentally determined yields for emission of F^-, F^+ and Li^+ secondary ions due to impact of Ar^{2+} and Ar^{9+} ions on LiF as a function of ion impact energy. Total sputter yields are plotted for comparison. Data from [17] (solid line for guidance only).

Table 1
Potential sputtering effect for different surface materials (cf. text)

Au	Metal	No
Si	Semiconductor	No
GaAs	Semiconductor	No
MgO	Insulator (oxyd)	No
SiO_2	Insulator (oxyd)	Yes
LiF	Insulator (alkalihalide)	Yes
NaCl	Insulator (alkalihalide)	Yes

tightly bound inner shells (e.g. *M*, *L*, *K*) are filled by Auger neutralisation from the conduction band or in close collisions with target atoms [20–24]. In this way, the potential energy of the projectile is converted into kinetic energy of emitted electrons and electronic excitation of a small surface region (creation of electron–hole pairs, "hot holes" in the conduction/valence band of the target, and inner-shell holes of target atoms). For metal surfaces such sudden perturbations of the electronic structure can be rapidly accommodated and the excitation energy will dissipate within the target material without inducing structural surface modification.

For insulator targets, however, such a strong electronic excitation might survive long enough and/or

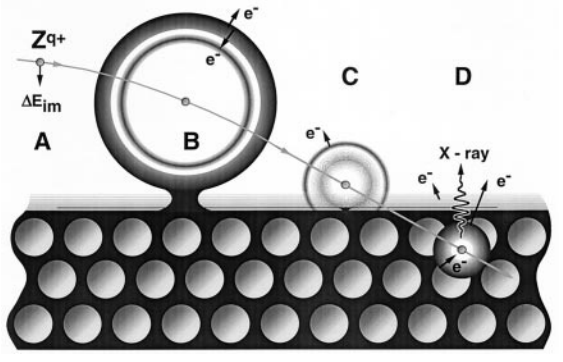

Fig. 10. Scenario for impact of a slow HCI on a surface. (A) The HCI approaches the surface by acquiring an image charge energy gain ΔE_{im}. (B) Formation of a hollow atom above the surface gives rise to electron emission, e.g. via autoionisation and Auger neutralization processes; the target surface becomes electronically excited. (C) Screening of the HA by surface electrons induces further electron emission. (D) The HA relaxes at/below the surface via emission of electrons and x rays. In certain target materials the electronic excitation of the target can lead to potential sputtering.

become efficiently converted into kinetic energy of desorbed or sputtered target atoms and ions. This is the origin of sputtering induced by the projectile's potential energy, i.e. PSI. Currently two competing models for such conversion processes are being considered, namely Coulomb explosion (CE) and defect mediated sputtering (DS), respectively. Both models predict correctly that sputtering of conducting targets (i.e. metal) should not depend on the projectile ion charge, i.e. only kinetic sputtering is possible.

In the CE model proposed by Parilis and coworkers [25,26] the neutralisation of a HCI impinging on an insulator surface is assumed to result in a strong electron depletion of the near surface region. Consequently, the mutual Coulomb repulsion of target ion cores gives rise to ejection of secondary ions from positively charged microscopic surface domains. Shock waves generated by the CE then ablate further target material (emission of neutral target atoms/clusters). In this way the CE model not only explains an enhanced secondary ion emission yield but also accounts for sputtering of neutrals which can strongly enhance the removal of surface material.

Recently, molecular dynamics (MD) simulations for CE processes in pure Si have been performed [27]. In these calculations the following CE scenario was assumed:

(1) The HCI–Si interaction leaves a half sphere containing 265 or more positively charged silicon ions on a Si (111) surface.

(2) The replenishment of electrons from the surrounding solid does not proceed rapidly enough, such that the repulsive electrostatic energy stored in the charged region leads to a Coulomb driven shock wave that eventually leaves a crater-like feature in the surface.

These MD calculations show that the shock wave needs about 100 fs to fully develop and the resulting crater formation time is about 1 ps. Moreover, the energy distribution of the emitted ions is rather broad, with a mean energy of about 100 eV.

In a different approach, PSI has been successfully explained [6] within a DS model. In certain insulator materials (alkali halides, SiO_2) electronic defects which are induced by bombardment with energetic

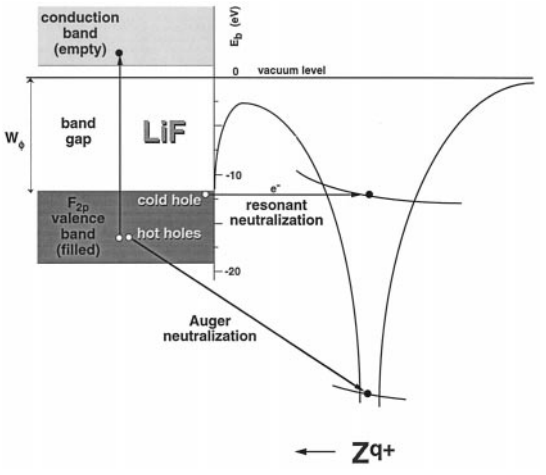

Fig. 11. Electronic transitions between surface and projectile ion leading to formation of holes (via resonant neutralization) as well as electron–hole pairs (via Auger neutralization).

electrons [electron-stimulated desorption (ESD)] as well as UV photons [photon-stimulated desorption (PSD)] can lead to sputtering [28–32]. As described above, strong interaction of a HCI with any target surface will cause formation of electron–hole pairs (via Auger neutralisation, cf. Fig. 11) as well as large number of holes (via resonant neutralization, cf. Fig. 11). Due to the strong electron–phonon coupling (i.e. efficient energy transfer from the electronic to the phononic system of the solid) in alkali halides and SiO_2, such an electronic excitation of the valence band will become localised by formation of "self-trapped excitons" (STE) and/or "self-trapped holes" (STH), i.e. excitons or holes trapped in a deformation of its own lattice [33,34], respectively (for a more detailed description for LiF targets cf. the following). As in the case of ESD/PSD, decay of such STH and/or STE into different "colour centers" (*H* and *F* centers in the case of alkali halides and *E′* centers in the case of SiO_2) leads to the desorption of neutralized anions (halide atoms, oxygen). In LiF, e.g., an *H* centre is a F_2^- molecular ion at one anion lattice site, while an *F* centre is an electron localised at the next or second-next anion site [33,34]. The such created neutral cations are either evaporated (as in the case of heated alkali halide samples) or can be removed by sufficient momentum transfer from the impinging projectiles.

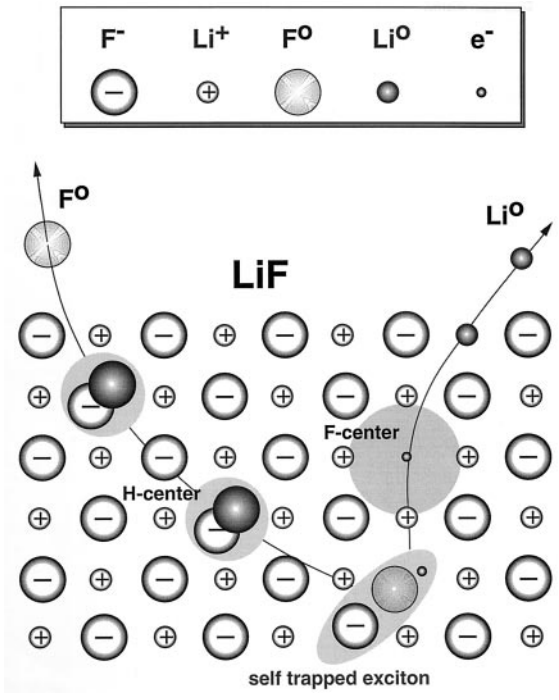

Fig. 12. The potential sputtering process explained according to the defect mediated sputtering model (cf. text). Negatively charged F^- and positively charged Li^+ ions of the ionic LiF crystal are shown as open circles. An electronic excitation (electron–hole pair) becomes localized as a self-trapped exciton (STE, lower right) which subsequently decays into colour (*H* and *F*) centers. These colour centers diffuse to the surface where they will cause the emission of neutral atoms (closed circles).

As an example, in Fig. 12 the PSI process for a LiF target surface is schematically depicted. If the HCI approaches the LiF surface, holes in the F(2*p*) valence band will be created by resonance neutralisation (RN). "Cold holes" (i.e. holes localised at the Fermi edge) in the first surface layer will form V_k centres (F_2^- molecular ions adjacent to two anion sites) [33,34], and the resulting highly excited projectiles become de-excited by Auger and autoionization processes, leading to electron emission. When the projectile penetrates the surface layer when still in an ionised or highly excited state, interatomic Auger neutralisation (AN) and RN will take place and further neutralise and/or de-excite the projectile, producing further electron–hole pairs. Hot holes will be formed with higher probability because of the larger electron density in the centre of the valence band. Therefore, resulting V_k centres can trap available electrons, thus forming STEs which at room temperature will immediately decay into two colour centres, i.e. an *H* centre (F_2^- molecular ion at one anion lattice site) and an *F* centre (electron localised at the next or second-next anion site) [33,34]. *H* and *F* centres created in the bulk can diffuse to the surface, where the *H* centre will decay by emitting an F^0 atom and the *F* centre can neutralise a Li^+ cation. For electron bombardment Li atoms created at the surface will form a metallic overlayer which eventually stops further progress of ESD or PSD at room temperature, but can be evaporated at surface temperatures above 150 °C. In contrast to ESD, even at rather low impact energy the much heavier HCI projectiles provide sufficient momentum transfer for removing single weakly (van der Waals) bound Li atoms from the LiF surface, which assures stoichiometric desorption already at low surface temperature.

Within the DS model of PSI it is not sufficient for a target surface to be an insulator. An enhancement of the absolute total sputter yields with increasing charge state of the primary ion is predicted only for targets with strong electron–phonon coupling, where electronic excitation can be localised by formation of STE and/or STH.

5. Discussion

The experimental evidence presented in Sec. 3 favours the defect mediated sputtering over the Coulomb explosion model. In the following we will summarize the main indications.

(1) Only for alkali halides (LiF, NaCl) [13] and to a weaker extent for SiO_2 [14,16] PSI has been observed so far. Both SiO_2 and alkali halides are materials which are known to exhibit strong electron–phonon coupling and STH or STE formation.

(2) All other target species investigated by the quartz crystal micro balance technique (Au, Si, GaAs, and MgO) show only kinetically induced sputtering up to the highest available Ar^{q+} charge state of $q = 9$ [14,15]. According to the CE model also insulators

like MgO and semiconductors like Si and GaAs should show a charge state dependence of the sputtering yield. However, no STH or STE formation is known for these materials. Without that property even in insulators the lifetime of valence band holes seems to be too short for developing enough repulsive energy by Coulomb forces.

(3) The electronic defects in the surface (e.g. number of electron–hole pairs and holes created) should be roughly proportional to the potential energy carried by the projectile into the surface. In the case of defect mediated sputtering the number of STHs and STEs and, in further consequence, the number of sputtered particles should therefore also increase nearly linear with the potential energy, as has been observed in experiment [13]. However, for the CE mechanism also a strong increase with the potential energy is to be expected.

(4) A CE process should favour the production of positively charged secondary ions while hampering the emission of negatively charged ions and electrons. At least for alkali-halide targets predominantly neutrals and less than 1% ions have been observed [17]. In secondary ion emission experiments with very highly charged ions (up to $q = 78$) on SiO_2 [35] negatively charged ions have been found to be as abundant as positively charged ones, which is difficult to reconcile with the notion of CE.

(5) At very low energy impact of Ar^{q+} ($q \leq 9$) on SiO_2, the effect of potential sputtering was found to decrease with increasing ion dose. According to the defect mediated sputtering model, the cations are removed by evaporation (alkali halides) or by momentum transfer from the impinging projectile to the now weakly bound (because neutralized) cation. In SiO_2 the removal of the cations is only possible by the latter mechanism (main difference between alkali halides and SiO_2). Therefore, at very low impact energies only oxygen is sputtered and the surface is enriched in Si. Consequently, the potential sputtering effect decreases with increasing ion dose. The same effect leads to the formation of a metallic Li overlayer in the case of ESD from LiF at low target temperatures [28]. An alternative explanation in terms of the CE model is not obvious.

(6) Additional evidence in favour of the DS model comes from the energy distribution of sputtered particles. The recent molecular dynamics simulation, which uses the CE mechanism as input for the initial conditions [27] predicts the ejection of energetic sputtered particles. In the numerical example of [27], the average energy was ≈4 a.u. (∼100 eV). This is in striking contrast to experimental findings of sputtered neutrals and ions whose overwhelming majority have low energies (≈ eV).

We conclude that trapping of electronic defects due to strong electron–phonon coupling is essential in mediating potential sputtering. However, conventional wisdom in electron- and photon-stimulated desorption considers primarily the formation of STE, their subsequent decay into an F and H pair and diffusion to the surface as mechanism for stoichiometric sputtering. Such a mechanism will also be operative for potential sputtering induced by slow highly charged ions when charge transfer proceeds by Auger capture. Due to the limited number of Auger capture events only a relatively small number of STEs can be produced. However, resonant capture which is more probable than Auger capture, creates only holes (the number of holes being roughly proportional to the charge state of the incoming projectile [1,19]). Unlike for photon- or electron-stimulated desorption, it is quite plausible that self-trapped holes are also important in potential sputtering by highly charged ions. While a self-trapped hole at the surface can result in sputtering of the neutral halide, the presence of a large number of electrons in the impact zone of a highly charged ion due to resonant reionization (“recycled electrons”), secondary electron emission and Auger deexcitation processes may account for the concomitant emission of neutral alkali atoms. The latter process is less likely for photon or electron stimulated desorption because a comparably strong source of electrons is lacking. Self-trapped holes as a new agent specific for potential ion-induced sputtering could also account for the fact that sputtering yields for Ar^+ are only 30%–50% of those for Ar^{2+}. Within the STE mechanism a much smaller ratio would be predicted since Ar^{2+} permits Auger capture and formation of excitons while Ar^+ carries insufficient potential en-

ergy for STE formation. On the other hand, Ar^{2+} will create about twice the number of holes than Ar^{+}, and the observed ratio of PSI yields is consistent with a STH induced sputtering process. The question whether STH formation alone can already induce potential sputtering is currently under investigation. Preliminary results indicate a PSI threshold for LiF at around 10 eV potential energy [36], which strongly supports the above presented arguments about the role of STH formation.

Acknowledgements

This work has been supported by Austrian Fonds zur Förderung der wissenschaftlichen Forschung and was carried out within Association EURATOM-ÖAW. The authors would like to thank J. Burgdörfer (TU Wien) for many valuable discussions. Fruitful collaborations with M. Schmid (TU Wien) and N. Stolterfoht (HMI Berlin), and participation of T. Neidhart, M. Sporn, D. Niemann, M. Grether, and G. Hayderer in various parts of the measurements are gratefully acknowledged.

References

[1] A. Arnau, F. Aumayr, P.M. Echenique, M. Grether, W. Heiland, J. Limburg, R. Morgenstern, P. Roncin, S. Schippers, R. Schuch, N. Stolterfoht, P. Varga, T.J.M. Zouros, HP. Winter, Surf. Sci. Rep. 229 (1997) 1.
[2] J. Burgdörfer, P. Lerner, F.W. Meyer, Phys. Rev. A 44 (1991) 5647.
[3] J. Burgdörfer, in Fundamental Processes and Applications of Atoms and Ions, C.D. Lin (Ed.), World Scientific, Singapore, 1993.
[4] F. Aumayr, HP. Winter, Comments At. Mol. Phys. 29 (1994) 275.
[5] F. Aumayr, in The Physics of Electronic and Atomic Collisions, L.J. Dubé, et al. (Eds.), AIP Press, Woodbury, NY, 1995, Vol. 360, p. 631.
[6] F. Aumayr, J. Burgdörfer, P. Varga, HP. Winter, Comments At. Mol. Phys. 34 (1999) 201.
[7] T. Neidhart, Z. Toth, M. Hochhold, M. Schmid, P. Varga, Nucl. Instrum. Methods Phys. Res. B 90 (1994) 496.
[8] C. McKeown, Rev. Sci. Instrum. 32 (1961) 133.
[9] O. Ellegard, J. Schou, H. Sorensen, P. Borgesen, Surf. Sci. 167 (1986) 474.
[10] IEEE Standard on Piezoelectricity, IEEE, New York, 1978, p. 176.
[11] E.P. EerNisse, J. Appl. Phys. 43 (1972) 1330.
[12] M. Leitner, D. Wutte, J. Brandstötter, F. Aumayr, HP. Winter, Rev. Sci. Instrum. 65 (1994) 1091.
[13] T. Neidhart, F. Pichler, F. Aumayr, HP. Winter, M. Schmid, P. Varga, Phys. Rev. Lett. 74 (1995) 5280.
[14] P. Varga, T. Neidhart, M. Sporn, G. Libiseller, M. Schmid, F. Aumayr, HP. Winter, Phys. Scr. T 73 (1997) 307.
[15] T. Neidhart, F. Pichler, F. Aumayr, HP. Winter, M. Schmid, P. Varga, 3S'95 Symposium on Surface Science, P. Varga, F. Aumayr (Eds.), Kitzsteinhorn, Salzburg, Austria, 1995, p. 74.
[16] M. Sporn, G. Libiseller, T. Neidhart, M. Schmid, F. Aumayr, HP. Winter, P. Varga, M. Grether, N. Stolterfoht, Phys. Rev. Lett. 79 (1997) 945.
[17] T. Neidhart, F. Pichler, F. Aumayr, HP. Winter, M. Schmid, P. Varga, Nucl. Instrum. Methods Phys. Res. B 98 (1995) 465.
[18] C. Lemell, HP. Winter, F. Aumayr, J. Burgdörfer, F.W. Meyer, Phys. Rev. A 53 (1996) 880.
[19] F. Aumayr, H. Kurz, D. Schneider, M.A. Briere, J.W. McDonald, C.E. Cunningham, HP. Winter, Phys. Rev. Lett. 71 (1993) 1943.
[20] S. Schippers, S. Hustedt, W. Heiland, R. Köhrbrück, J. Kemmler, D. Lecler, N. Stolterfoht, in Ionization of Solids by Heavy Particles, R. Baragiola (Ed.), Plenum, New York, 1993, Vol. 306, p. 117.
[21] N. Stolterfoht, A. Arnau, M. Grether, R. Köhrbrück, A. Spieler, R. Page, A. Saal, J. Thomaschewski, J. Bleck-Neuhaus, Phys. Rev. A 52 (1995) 445.
[22] A. Arnau, P.A. Zeijlmans van Emmichoven, J.I. Juaristi, E. Zaremba, Nucl. Instrum. Methods Phys. Res. B 100 (1995) 279.
[23] A. Arnau, R. Köhrbrück, M. Grether, A. Spieler, N. Stolterfoht, Phys. Rev. A 51 (1995) R3399.
[24] J. Burgdörfer, C. Reinhold, F. Meyer, Nucl. Instrum. Methods Phys. Res. B 98 (1995) 415.
[25] I.S. Bitensky, E.S. Parilis, J. Phys. (Paris) C 2 (1989) 227.
[26] I.S. Bitenskii, M.N. Murakhmetov, E.S. Parilis, Sov. Phys. Tech. Phys. 24 (1979) 618.
[27] H.P. Cheng, J.D. Gillaspy, Phys. Rev. B 55 (1997) 2628.
[28] M. Szymonski, A. Poradzisz, P. Czuba, J. Kolodziej, P. Piatkowski, J. Fine, L. Tanovic, N. Tanovic, Surf. Sci. 260 (1992) 295.
[29] M. Szymonski, in Fundamental Processes in Sputtering of Atoms and Molecules, P. Sigmund (Ed.), Royal Danish Academy of Sciences, Copenhagen, 1993, p. 495.
[30] N. Seifert, D. Liu, A. Barnes, R. Albridge, Q. Yan, N. Tolk, W. Husinsky, G. Betz, Phys. Rev. B 47 (1993) 7653.
[31] R.E. Walkup, P. Avouris, A. Ghosh, Phys. Rev. B 36 (1987) 4577.
[32] T. Green, Phys. Rev. B 35 (1987) 781.
[33] R. Williams, Phys. Rev. B 33 (1986) 7232.
[34] R. Williams, K. Song, J. Phys. Chem. 51 (1990) 679.
[35] D.H. Schneider, M.A. Briere, J. McDonald, J. Biersack, Rad. Eff. Def. Solids 127 (1993) 113.
[36] G. Hayderer et al., unpublished.